

Single-Cell Imaging Approaches for Studying Small-RNA-Induced Gene Regulation

Hye Ran Koh^{1,2} and Sua Myong^{1,3,*}

¹T.C. Jenkins Department of Biophysics, Johns Hopkins University, Baltimore, Maryland; ²Department of Chemistry, Chung-Ang University, Seoul, Korea; and ³Department of Physics, Center for the Physics of Living Cells and Institute for Genomic Biology, University of Illinois at Urbana-Champaign, Urbana, Illinois

ABSTRACT RNA interference (RNAi) is a process by which gene expression is downregulated by small interfering RNAs or microRNAs. The quantification of the RNAi efficiency can be performed at both the messenger RNA (mRNA) and the protein level, which is required to assess the potency of small interfering RNAs or microRNAs. Recently, we employed a single-cell mRNA imaging method to study RNAi in which we visualized individual mRNA targets with high precision while resolving the cellular localization and cell-to-cell heterogeneity in addition to RNAi efficiency. In this Biophysical Perspective, we highlight our recent work on quantitative analysis of the RNAi pathway and point out some important future directions. Alongside, we discuss about several single-cell imaging techniques that can be applied to study RNAi. The single-cell imaging techniques discussed here are widely applicable to other gene regulation processes such as the CRISPR-CAS system.

RNA interference (RNAi) is a multistep cellular process in which small RNAs in the form of small interfering RNAs (siRNAs) or microRNAs (miRNAs) inhibit the target gene in a sequence-specific manner (by complementary base pairing). Since Craig Mello and Andrew Fire noticed the potential of RNAi as a tool to silence a specific gene (1), RNAi has been widely employed for functional genetic studies (2,3) as well as the development of genetic therapies (4–6) owing to its power to downregulate specific genes of interest. Extensive biochemical and structural studies have uncovered detailed molecular mechanisms that underpin this intricate regulatory pathway (7–12). Despite its clear advantages, the usage of RNAi has been greatly limited due to problems such as the off-target effect and other factors that reduce the efficiency of gene silencing (13,14).

The RNAi pathway involves well-documented stepwise reactions, as shown in Fig. 1, starting from the binding of precursor siRNAs or miRNAs (pre-siRNAs or pre-miRNAs) by the double-strand RNA (dsRNA)-cleaving enzyme, Dicer, and its cofactor, TAR-RNA binding protein (TRBP). Dicer/TRBP cleaves the pre-siRNA or pre-miRNA, producing the shorter and mature dsRNA, siRNA, or miRNA of 21–23 base pairs, in which one strand is

selected by the ternary protein complex consisting of Argonaute (Ago), Dicer, and TRBP, termed RNA-induced silencing complex. Subsequently, the Ago incorporated with the selected single-strand RNA (ssRNA) finds the complementary target messenger RNA (mRNA), resulting in the cleavage of the target mRNA or the translational inhibition without cleaving it. In both cases, the target protein cannot be produced. In short, RNAi is the process by which a small RNA inhibits the expression of the target protein (Fig. 1 B). We envision that direct imaging and quantitation of the small RNAs, the target mRNA, and/or the protein would contribute to providing a comprehensive view of the RNAi process.

Here, we discuss how to study RNAi by imaging small RNAs, the target mRNA, and the target protein at the single-cell level. Unlike the conventional approaches in this field, the single-cell imaging approaches to tackle the molecular mechanism of RNAi provide characteristics of RNAi that can be masked when measured at the ensemble level, such as cellular localization of the small RNAs and target gene as well as cell-to-cell heterogeneity. Recently, various research on RNAi based on single-cell imaging approaches was reported. Visualization of the target mRNAs and their constituent proteins showed that Ago2 and other processing body components colocalize with the target mRNA after 24 hr of miRNA induction, indicating the long-term storage of miRNA-regulated mRNA by the recruitment of processing body components (15). Visualization of miRNAs at single-molecule resolution revealed two

Submitted April 4, 2018, and accepted for publication May 24, 2018.

*Correspondence: smyong@jhu.edu

Editor: Antoine van Oijen.

<https://doi.org/10.1016/j.bpj.2018.05.040>

© 2018 Biophysical Society.



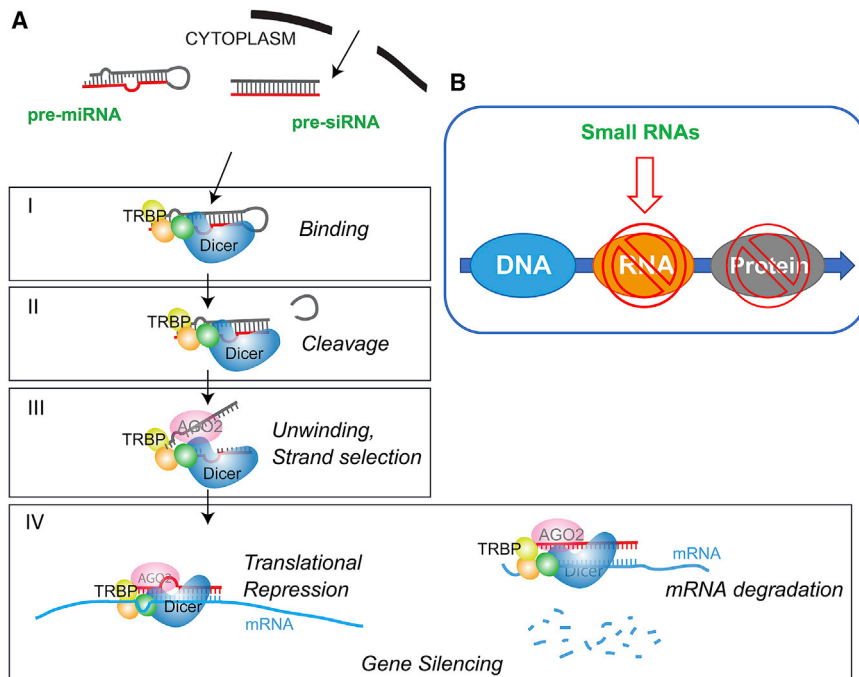


FIGURE 1 The molecular mechanism of RNAi. (A) The stepwise gene-silencing pathway induced by small RNAs consists of 1) Dicer/TRBP binding to small RNAs, pre-siRNA, or pre-miRNA; 2) the cleavage of pre-siRNA or pre-miRNA by Dicer/TRBP, producing siRNA or miRNA; 3) strand selection of siRNA or miRNA by the Ago, Dicer, and TRBP complex; and 4) the inhibition of target mRNA and protein. (B) In RNAi, small RNAs induce the cleavage of the target mRNA, resulting in the repression of target protein expression, or inhibit the translation of target protein without cleaving target mRNA. Both cases result in the repression of the target protein. To see this figure in color, go online.

distinct miRNA assembly pathways and the enhancement of nuclear retention of mature miRNAs by seed-matched target mRNA (16,17). Degradation of mRNAs was also visualized by engineering a single-mRNA turnover, showing that siRNA-treated mRNA is rapidly degraded in the cytoplasm (18). Our recent work that visualized the target mRNAs and target proteins focuses on the quantification of target mRNA by screening various structures of siRNA/miRNA, suggesting that the mismatches of siRNA/miRNA control the silencing pathway kinetically (19). We discuss single-cell imaging approaches to study RNAi, focusing on our recent work, and their future direction in this field.

Cellular imaging of the small RNAs upon RNAi

The small RNAs that induce gene silencing can be categorized as siRNA and miRNA based on their origin. The siRNA is typically an exogenous RNA that can be inserted into cells, whereas the miRNA is an endogenous source of small RNAs that are genome encoded and transcribed by RNA polymerase II. In other words, the siRNAs can be engineered before their insertion into cells, but it is not possible to change miRNAs that already exist in cells. siRNA often refers to short perfect dsRNA of ~21 bp in length with 2-nt 3' overhang at both ends; however, we will use the term siRNAs more generally to include all exogenous small RNAs with various structures that are capable of inhibiting their target gene. For example, they include the ssRNAs of 21–23 nt and the short dsRNAs of 21–23 bp that do not require cleavage by Dicer/TRBP (Dicer product) and the dsRNAs longer than 21–23 bp that require dicing (Dicer substrate). We will not consider dsRNAs longer than 30 bp

in this Perspective because such RNAs may induce innate immune response in mammalian cells (20).

To visualize siRNAs in cells, the easiest approach is to label the siRNAs with fluorophores, transfect them into cells, and image them using a fluorescence microscope. One-color or two-color labeling strategy has been tried for imaging siRNAs at single-cell level (21,22). The two-color labeling approach can be in the form of fluorescence resonance energy transfer (FRET), which enables distinguishing the dsRNA (FRET) from the ssRNAs (no FRET), or simple two-color labeling, which differentiates dsRNA (colocalization) and ssRNA (no colocalization) (22). For both approaches, it is critical to choose proper labeling positions and fluorophores because any chemical modification of siRNAs could significantly reduce their silencing capability (23). The duplex form of siRNAs consists of a guide strand and a passenger strand, in which the guide strand is recruited to the RNA-induced silencing complex to inhibit the target gene while the passenger strand is ejected and removed. The 5' phosphorylation of the guide strand is required for the target mRNA cleavage (24), whereas the 3' end structure of siRNA modulates the Dicer cleavage (25). Therefore, it is critical to avoid modifying and labeling these positions for siRNA visualization. It is recommended to label the internal position (within the duplex stem) or the loop region for siRNAs with a stem-loop structure. We designed our RNA with an amine-modified uracil at the intended labeling position during the chemical synthesis of the siRNAs and labeled these modified siRNAs with N-hydroxysuccinimide (NHS) ester-modified fluorophores (Fig. 2).

Next, we should insert the engineered siRNAs into cells to visualize them. Various approaches have been proposed

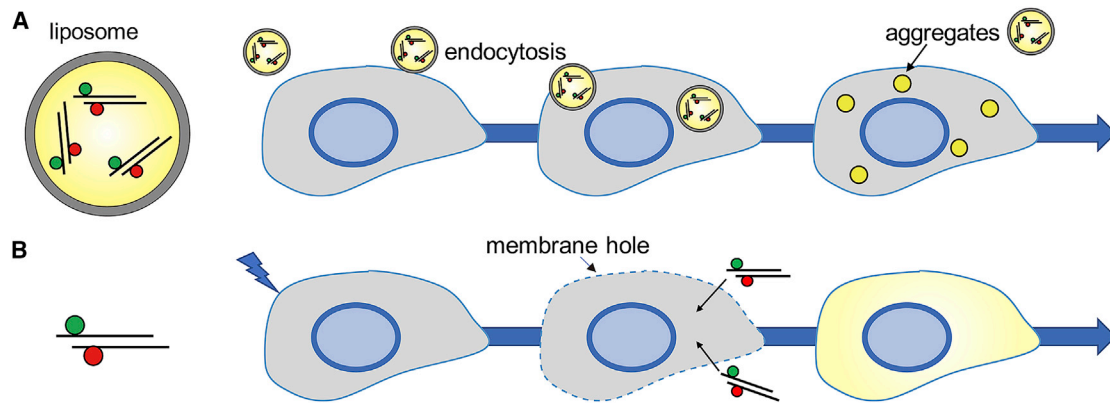


FIGURE 2 The small RNA imaging during RNAi shows its localization depending on delivery methods. Visualization of small RNAs would provide the information of the different delivery methods of small RNAs. (A) The liposome-based delivery of small RNAs would show the aggregates of small RNAs due to the encapsulation of the multiple small RNAs in one liposome. (B) Electroporation or microinjection of small RNAs would initially show the homogeneous distribution of small RNAs due to their direct delivery. To see this figure in color, go online.

to deliver the siRNAs into cells or tissues with the goal of delivering siRNAs to specific cells, such as cancer cells, as genetic drugs (26). Imaging siRNAs can be a direct means of checking for the siRNA delivery. The labeled siRNAs can be easily visualized using the conventional fluorescence microscope. We note that advanced fluorescence microscopy such as a single-molecule fluorescence microscope is required to resolve single siRNA molecules. After delivering labeled siRNAs into cells using liposome-based transfection, we observed aggregation of siRNAs (Fig. 2 A), as expected from siRNAs being captured in liposomes and taken up by cells via endocytosis. However, with different delivery methods, such aggregation may not take place (Fig. 2 B). Taken together, the visualization of siRNAs provides information about the efficiency of siRNA delivery and the localization of the siRNAs over time after the delivery at the single-cell level, which cannot be achieved by the conventional quantification of the siRNAs based on gel-electrophoresis-based assays.

Cellular imaging of the target mRNA upon RNAi

RNAi reduces gene expression in two pathways, transcriptional inhibition and translation repression, and the visualization of the target mRNA reveals which pathway is chosen in a direct manner. For example, if the translational repression is the dominant pathway, the target mRNA will not be reduced in number after siRNA uptake. A significant advantage of the mRNA visualization at the single-cell level is that the nuclear mRNA can be clearly distinguished from the cytoplasmic mRNA due to the spatial separation of the two compartments. The single-molecule in situ hybridization (smFISH) was developed to visualize mRNA at the single-cell level on fixed cell samples, where multiple DNA probes can be designed and applied to hybridize to one specific target mRNA, making the target mRNA substantially brighter far above the fluorescence background induced by

nonspecific binding (27). The brightness enables one to count the number of mRNA in individual cells (nuclear versus cytoplasmic) with high precision (27).

To monitor the target mRNAs upon RNAi treatment at the single-cell level, we fixed the cells (HEK293 or HeLa) over the time course (0, 1, 2, 3, 4, and 6 hr) after the siRNA transfection (19). We then hybridized DNA FISH probes. As shown in Fig. 3 A, we observed abundant bright signals arising from individual mRNA targets before RNAi treatment. After the addition of siRNAs, mRNA molecules can be cleaved into two fragments that may appear dimmer in fluorescence intensity if the cleavage position is located within the FISH probe binding region and if the cells were fixed when this occurred. However, immediately after the cleavage event, each fragment of the target mRNA is expected to be cleaved by the cellular mRNA decay process such as 5'→3' exonucleases and 3'→5' exonucleases (28,29). As a result, in most cases, the DNA probes cannot be hybridized to the target mRNAs at all because they are fully degraded, resulting in no fluorescence rather than dim signal. Therefore, counting the number of the target mRNAs over time after the siRNA delivery would give the kinetics of the gene silencing at the single-mRNA and single-cell level (Fig. 3 B) (19).

Despite the high resolution and precision of mRNA images provided by the smFISH, it is limited only to fixed cells. Therefore, tracking the mRNAs over time after the siRNA delivery in real time would provide a more accurate view of the fate of the target mRNAs upon RNAi treatment. For this, visualization of the target mRNAs in live cells is necessary. Many live-cell mRNA-imaging approaches, including the MS2-GFP system that can be established by genetically encoded fluorescent tags in live cells (30) and the RNA spinach system, have been developed and widely applied (31,32). But we should keep in mind that the engineered target mRNAs can distort the kinetics of RNAi. A recent study based on imaging target mRNAs in live cells

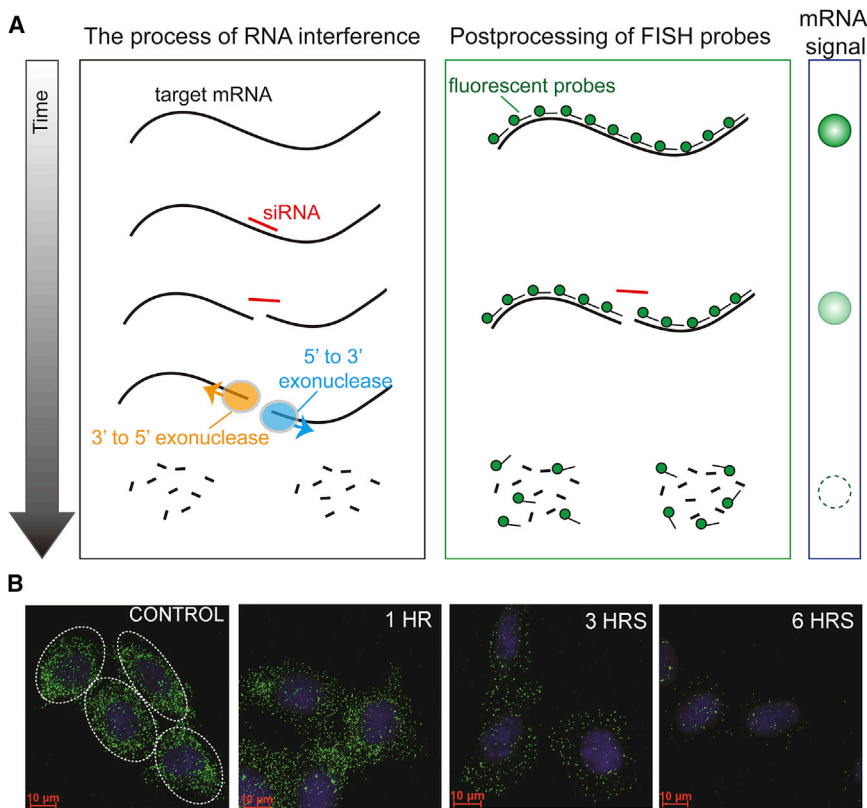


FIGURE 3 The mRNA imaging during RNAi using smFISH in fixed cells. (A) The fate of target mRNA during RNAi pathway and how to detect target mRNA by smFISH is shown. (B) The representative images of lmnA mRNAs over the time course after the induction of lmnA siRNA are shown. Each green dot displays a single lmnA mRNA, and each blue circle the nucleus. To see this figure in color, go online.

showed that RNAi could occur in the nucleus as well as the cytoplasm, in contrast to the previous reports (33). The study used a designed gene construct with an inducible promoter that encodes a combined transcript and 3'UTR containing multiple MS2 binding sequence repeats. Subsequently, the MS2 sequence can be coated with GFP-MS2 fusion protein, enabling visualization of the engineered target mRNA. There are several live-cell mRNA-imaging techniques that do not require the engineering of the target mRNAs, such as the mRNA-capturing DNA probes resembling the smFISH (34). Even in this case, we should be careful about interpreting the effect of RNAi because the mRNA-capturing DNA probes can play a role in protecting the single-stranded target mRNA, preventing mRNA degradation and distorting the RNAi kinetics.

Cellular imaging of the target protein upon RNAi

In most cases, the ultimate goal of using RNAi in biology is to reduce the target proteins, not the target mRNAs. Therefore, the quantification of the target protein upon RNAi is an essential readout of RNAi. Unlike other protein quantification methods such as immunoprecipitation, direct visualization of the target proteins in cells provides the spatial localization of the protein in the cells in the course of RNAi. We employed the immunostaining method to visualize our target protein, lmnA, which is one of the architec-

tural proteins that sustains the nuclear envelope (Fig. 4 A). One of two immunostaining methods, the direct method or the indirect method, could be employed to visualize the target proteins. The direct method uses a fluorescently labeled primary antibody that interacts with the target proteins, whereas the indirect method uses an unlabeled primary and a labeled secondary antibody that interacts with the primary antibody against our target proteins for their visualization.

To study the RNAi effect of lmnA, we visualized lmnA protein after introducing siRNAs for the lmnA gene. The cells were fixed at different times after siRNA treatment against lmnA, and the primary antibody and Cy5-labeled secondary antibody were applied. Under the fluorescence microscope, lmnA protein was visualized as shown in Fig. 4 B, and we quantified the protein level by measuring the fluorescence intensity. Due to the single-cell resolution, we were able to observe the highly heterogeneous nature of protein reduction from cell to cell as shown in Fig. 4 C, in which one triangle indicates the average lmnA protein level of an individual cell. Interestingly, we found that the protein reduction (red triangle in Fig. 4 C) is ~30 hr delayed from the mRNA reduction (black triangle). Such delay can be due to the long lifetime or the slow turnover of the lmnA protein (Fig. 4 C) (35). In other words, even though the mRNA is degraded by the RNAi mechanism (hence no more synthesis of new proteins), the pre-existing proteins can be sustained until the moment of

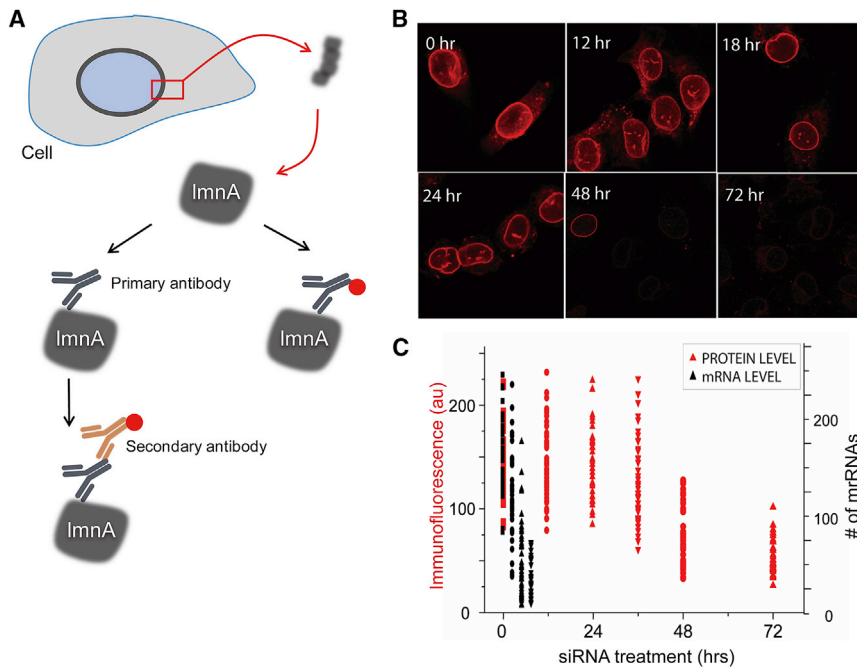


FIGURE 4 The target protein imaging during RNAi using immunostaining. (A) The immunostaining methods to visualize ImnA proteins that localize at the nuclear membrane are shown. The indirect method visualizes the fluorophore-labeled (displayed as a red circle) secondary antibody that interacts with the primary ImnA antibody, and the direct method visualizes the fluorophore-labeled primary ImnA antibody. (B) The representative images of ImnA proteins using the indirect method show the perinuclear localization of ImnA proteins and their reduction over time after the induction of ImnA siRNA. (C) The comparison of the reduction kinetics between the mRNA level and protein level of ImnA after the induction of ImnA siRNA is shown. The left y axis is for the protein level, and the right y axis for the mRNA level. To see this figure in color, go online.

cell division, during which the nuclear wall has to break down, for example. This result suggests that RNAi is a fast-acting mechanism that occurs in the time course of 1–6 hr post-siRNA entry into cells, and the corresponding reduction in protein level can be delayed for many hours due to the stability of the pre-existing protein. Therefore, measuring the mRNA level but not the protein level is ideally suited for testing the silencing efficiency and potency of different siRNA substrates as we have done in our study.

Application to the neuronal system

We discussed the single-cell imaging approaches to investigating the RNAi pathway by visualizing siRNAs, target mRNAs, and the target protein. We showed that the gene-silencing kinetics can be studied by using HeLa and A549 cells. The spatial separation of target mRNA allowed us to measure RNAi efficiency in nucleus versus cytoplasm. Such capability of localizing mRNA can be highly beneficial to studies of neurons, in which certain mRNA is either kept near the cell body or delivered to particular locations along the neuronal axis (36). Testing the RNAi effect in various locations of neurite will be an interesting future endeavor. In mammalian cell lines, we found that the disappearance of the target mRNA induced by RNAi was uniformly distributed in cytoplasm, likely due to the uniform distribution of the target mRNA for these cell lines (19). But this may not hold for the nerve cells because of their complex organization consisting of a cell body and a long axonal process (37,38). In light of the recent studies of neurodegenerative diseases, it will be intriguing to localize

mRNA transcripts implicated with diseases and study how or if RNAi occurs differently along the neuron as well as between neuronal cells. In addition, the application of the single-cell imaging approaches to study RNAi at the tissue level would be challenging but critical to understanding RNAi in a setting more relevant for clinical platforms.

AUTHOR CONTRIBUTIONS

Both authors conceived the idea and wrote the manuscript.

ACKNOWLEDGMENTS

This work was supported by the American Cancer Society (RSG-12-066-01-DMC), National Institutes of Health (IDP2 GM105453), National Institutes of Health (R01 GM115631), and National Science Foundation Physics Frontiers Center Program (0822613) through the Center for the Physics of Living Cells.

REFERENCES

1. Fire, A., S. Xu, ..., C. C. Mello. 1998. Potent and specific genetic interference by double-stranded RNA in *Caenorhabditis elegans*. *Nature*. 391:806–811.
2. Cullen, L. M., and G. M. Arndt. 2005. Genome-wide screening for gene function using RNAi in mammalian cells. *Immunol. Cell Biol.* 83:217–223.
3. Kamath, R. S., A. G. Fraser, ..., J. Ahringer. 2003. Systematic functional analysis of the *Caenorhabditis elegans* genome using RNAi. *Nature*. 421:231–237.
4. Thomas, C. E., A. Ehrhardt, and M. A. Kay. 2003. Progress and problems with the use of viral vectors for gene therapy. *Nat. Rev. Genet.* 4:346–358.

5. Pai, S. I., Y. Y. Lin, ..., T. C. Wu. 2006. Prospects of RNA interference therapy for cancer. *Gene Ther.* 13:464–477.
6. Bumcrot, D., M. Manoharan, ..., D. W. Sah. 2006. RNAi therapeutics: a potential new class of pharmaceutical drugs. *Nat. Chem. Biol.* 2:711–719.
7. Hannon, G. J. 2002. RNA interference. *Nature.* 418:244–251.
8. Schirle, N. T., and I. J. MacRae. 2012. The crystal structure of human Argonaute2. *Science.* 336:1037–1040.
9. Bernstein, E., A. A. Caudy, ..., G. J. Hannon. 2001. Role for a bidentate ribonuclease in the initiation step of RNA interference. *Nature.* 409:363–366.
10. Hammond, S. M., S. Boettcher, ..., G. J. Hannon. 2001. Argonaute2, a link between genetic and biochemical analyses of RNAi. *Science.* 293:1146–1150.
11. Song, J. J., S. K. Smith, ..., L. Joshua-Tor. 2004. Crystal structure of Argonaute and its implications for RISC slicer activity. *Science.* 305:1434–1437.
12. Macrae, I. J., K. Zhou, ..., J. A. Doudna. 2006. Structural basis for double-stranded RNA processing by Dicer. *Science.* 311:195–198.
13. Jackson, A. L., S. R. Bartz, ..., P. S. Linsley. 2003. Expression profiling reveals off-target gene regulation by RNAi. *Nat. Biotechnol.* 21:635–637.
14. Birmingham, A., E. M. Anderson, ..., A. Khvorova. 2006. 3' UTR seed matches, but not overall identity, are associated with RNAi off-targets. *Nat. Methods.* 3:199–204.
15. Shih, J. D., Z. Waks, ..., P. A. Silver. 2011. Visualization of single mRNAs reveals temporal association of proteins with microRNA-regulated mRNA. *Nucleic Acids Res.* 39:7740–7749.
16. Pitchiaya, S., J. R. Androsavich, and N. G. Walter. 2012. Intracellular single molecule microscopy reveals two kinetically distinct pathways for microRNA assembly. *EMBO Rep.* 13:709–715.
17. Pitchiaya, S., L. A. Heinicke, ..., N. G. Walter. 2017. Resolving subcellular miRNA trafficking and turnover at single-molecule resolution. *Cell Rep.* 19:630–642.
18. Horvathova, I., F. Voigt, ..., J. A. Chao. 2017. The dynamics of mRNA turnover revealed by single-molecule imaging in single cells. *Mol. Cell.* 68:615–625.e9.
19. Koh, H. R., A. Ghanbariniaki, and S. Myong. 2017. RNA stem structure governs coupling of dicing and gene silencing in RNA interference. *Proc. Natl. Acad. Sci. USA.* 114:E10349–E10358.
20. Gantier, M. P., and B. R. Williams. 2007. The response of mammalian cells to double-stranded RNA. *Cytokine Growth Factor Rev.* 18:363–371.
21. Vader, P., L. J. van der Aa, ..., R. M. Schifflers. 2010. A method for quantifying cellular uptake of fluorescently labeled siRNA. *J. Control. Release.* 148:106–109.
22. Järve, A., J. Müller, ..., M. Helm. 2007. Surveillance of siRNA integrity by FRET imaging. *Nucleic Acids Res.* 35:e124.
23. Hirsch, M., D. Strand, and M. Helm. 2012. Dye selection for live cell imaging of intact siRNA. *Biol. Chem.* 393:23–35.
24. Nykänen, A., B. Haley, and P. D. Zamore. 2001. ATP requirements and small interfering RNA structure in the RNA interference pathway. *Cell.* 107:309–321.
25. Kim, D. H., M. A. Behlke, ..., J. J. Rossi. 2005. Synthetic dsRNA Dicer substrates enhance RNAi potency and efficacy. *Nat. Biotechnol.* 23:222–226.
26. Whitehead, K. A., R. Langer, and D. G. Anderson. 2009. Knocking down barriers: advances in siRNA delivery. *Nat. Rev. Drug Discov.* 8:129–138.
27. Raj, A., P. van den Bogaard, ..., S. Tyagi. 2008. Imaging individual mRNA molecules using multiple singly labeled probes. *Nat. Methods.* 5:877–879.
28. Valencia-Sanchez, M. A., J. Liu, ..., R. Parker. 2006. Control of translation and mRNA degradation by miRNAs and siRNAs. *Genes Dev.* 20:515–524.
29. Orban, T. I., and E. Izaurralde. 2005. Decay of mRNAs targeted by RISC requires XRN1, the Ski complex, and the exosome. *RNA.* 11:459–469.
30. Bertrand, E., P. Chartrand, ..., R. M. Long. 1998. Localization of ASH1 mRNA particles in living yeast. *Mol. Cell.* 2:437–445.
31. Paige, J. S., K. Y. Wu, and S. R. Jaffrey. 2011. RNA mimics of green fluorescent protein. *Science.* 333:642–646.
32. You, M., and S. R. Jaffrey. 2015. Structure and mechanism of RNA mimics of green fluorescent protein. *Annu. Rev. Biophys.* 44:187–206.
33. Avivi, S., A. Mor, ..., Y. Shav-Tal. 2017. Visualizing nuclear RNAi activity in single living human cells. *Proc. Natl. Acad. Sci. USA.* 114:E8837–E8846.
34. Bao, G., W. J. Rhee, and A. Tsourkas. 2009. Fluorescent probes for live-cell RNA detection. *Annu. Rev. Biomed. Eng.* 11:25–47.
35. Cambridge, S. B., F. Gnad, ..., M. Mann. 2011. Systems-wide proteomic analysis in mammalian cells reveals conserved, functional protein turnover. *J. Proteome Res.* 10:5275–5284.
36. Lin, A. C., and C. E. Holt. 2007. Local translation and directional steering in axons. *EMBO J.* 26:3729–3736.
37. Murashov, A. K., V. Chintalgattu, ..., M. R. Van Scott. 2007. RNAi pathway is functional in peripheral nerve axons. *FASEB J.* 21:656–670.
38. Baudet, M. L., K. H. Zivraj, ..., C. E. Holt. 2011. miR-124 acts through CoREST to control onset of Sema3A sensitivity in navigating retinal growth cones. *Nat. Neurosci.* 15:29–38.